Frozen-in anticyclones occurring in polar Northern Hemisphere during springtime: Characterization, occurrence and link with quasi-biennial oscillation

Rémi Thiéblemont, Nathalie Huret, Y. J. Orsolini, Alain Hauchecorne, M.-A. Drouin

Frozen-in anticyclones occurring in polar Northern Hemisphere during springtime: Characterization, occurrence and link with quasi-biennial oscillation

R. Thiéblemont,[1] N. Huret,[1] Y. J. Orsolini,[2] A. Hauchecorne,[3] and M.-A. Drouin[1]

Received 30 March 2011; revised 13 July 2011; accepted 18 July 2011; published 20 October 2011.

[1] During winter, the polar vortex forms a dynamical barrier in the arctic stratosphere which prevents large scale exchanges between the high latitude and tropical regions. Nevertheless, the occurrence of thin tropical air mass intrusions at the edge of the polar vortex have in fact been detected and modeled. These structures could play an important role in improving our knowledge of the balance between chemical and dynamical processes associated with the ozone budget. After the final stratospheric warming in springtime, the breakdown of the polar vortex occurs and the summer circulation starts to develop. Air mass intrusions from the tropics can be trapped at polar latitudes and persist until August in the anticyclone, advected by summer easterlies. These structures, named "frozen-in anticyclones" (FrIACs), have already been observed in 2003 and 2005 by MIPAS-ENVISAT and MLS-AURA tracer measurements. We present here a new case of FrIAC in 2007 highlighted using MLS-AURA measurements. In order to better understand the dynamical conditions required for such events and the associated processes, we performed a climatology of tropical air mass intrusions using a potential vorticity contour advection model. This climatology reveals a preferred path for exchanges between the polar and tropical stratospheres. Using ERA-Iterim wind and temperature reanalysis from ECMWF, we have established links between FrIAC occurrences and Rossby wave activity. There is evidence that FrIACs can exist if no major sudden stratospheric warming occurs during the polar vortex phase and their development seems favorable if the tropical quasi-biennial oscillation is in the easterly phase.

Citation: Thiéblemont, R., N. Huret, Y. J. Orsolini, A. Hauchecorne, and M.-A. Drouin (2011), Frozen-in anticyclones occurring in polar Northern Hemisphere during springtime: Characterization, occurrence and link with quasi-biennial oscillation, *J. Geophys. Res.*, *116*, D20110, doi:10.1029/2011JD016042.

1. Introduction

[2] The ozone budget at high latitudes depends critically on the balance between transport and chemical (in gaseous or heterogeneous phase) processes. Tropical air slowly ascends in the upward branch of the Brewer-Dobson circulation and remains to some extent isolated from higher latitudes. However, many observations have revealed much faster transport out of the tropics and midlatitudes [*Ray et al.*, 1999; *Waugh*, 1996] with different amplitudes depending on the season [*Hoor et al.*, 2002]. The persistence of these intrusions at polar latitudes during winter leads to the development of low ozone pockets (LOPs) [*Manney et al.*, 1995; *Harvey et al.*, 2008]. There is great interest in improving our understanding of how and where air masses are transported from the tropics to higher latitudes much more rapidly than predicted by the Brewer-Dobson circulation process. Such fast transport of chemical compounds could have great impact on the stratospheric ozone budget at high latitudes [*Lahoz et al.*, 2007].

[3] The Arctic polar vortex breakdown during the final warming marks the onset of a westward summer circulation. However, air masses mix rather slowly in the summer stratosphere, and long-lived winter vortex remnants [*Durry and Hauchecorne*, 2005], tropical intrusions to high latitudes [*Huret et al.*, 2006], and "frozen-in" anticyclones [*Manney et al.*, 2006b] have been reported. Using the SLIMCAT chemical transport model, *Orsolini* [2001] showed that vortex air masses remain in the summer polar stratosphere until August but stated that additional measurements are required to confirm this finding. Using satellite measurements of N_2O from the Earth Observing System Microwave Limb Sounder (EOS-MLS), *Manney et al.* [2006b] revealed residual polar vortex air masses that were well identified spatially until at least mid-July in 2005 which

[1]Laboratoire de Physique et Chimie de l'Environnement et de l'Espace/CNRS, Université d'Orléans, Orleans, France.
[2]Norwegian Institute for Air Research, Kjeller, Norway.
[3]Laboratoire Atmosphères, Milieux, Observations Spatiales, Guyancourt, France.

0148-0227/11/2011JD016042

partly confirmed the calculations by *Orsolini* [2001]. They also identified long-lived "frozen-in" anticyclones (hereinafter referred as FrIACs) circling the pole, and originating from lower latitudes. *Lahoz et al.* [2007] presented a new picture of the spring and summer polar stratosphere using along-track measurements by the MIPAS instrument onboard the ENVISAT satellite. They further identified FrIACs in CH_4 MIPAS data for the year 2003. The paper of *Allen et al.* [2011] investigates the 2005 FrIAC case. They used a hierarchy of 2D (isentropic) and 3D models in order to describe and understand the evolution of FrIACs. These studies have improved our knowledge of dynamical conditions in the polar region during spring and summer and addressed the following question: "*how common are FrIAC occurrences?*." Besides this question of their occurrence, the processes responsible for such events have been investigated in the present paper.

[4] This study focuses on FrIAC occurrences and interannual variability to examine the processes driving such events. We use satellite data obtained by the Microwave Limb Sounder (MLS, V2.2) instrument from 2005 to 2009. We also perform simulations with the potential vorticity contour advection model "Modèle Isentrope de transport Méso-échelle de l'Ozone Stratosphérique par Advection" (MIMOSA) [*Hauchecorne et al.*, 2002] for the 850 K surface (~31 km), over the 2000–2009 period to build a climatology of FrIACs. The simulations have been performed using the horizontal winds, pressure and temperature fields provided by the ERA-Interim reanalysis [*Dee et al.*, 2011] from the European Center for Medium-Range Weather Forecast (ECMWF).

[5] Section 2 of the paper is dedicated to describing the tools used in this study. In Section 3, a new FrIAC event occurring in spring 2007 is reported and characterized. The dynamical state of the stratosphere as well as its evolution during springtime is compared for the three years with FrIAC events (2003, 2005 and 2007). Section 4 is devoted to the identification of the favorable dynamical conditions for the development of FrIACs: i) Rossby wave activity, ii) the occurrence of sudden stratospheric warmings, and iii) the phase of the quasi-biennial oscillation (QBO) in the tropical region. Finally, in Section 5 we summarize our analysis highlighting processes responsible for the FrIAC occurrences.

2. Tools

2.1. Chemical and Temperature Data From EOS MLS Instrument

[6] The MLS instrument onboard the Earth Observing System (EOS) Aura satellite observes the millimeter and sub-millimeter thermal emissions from the limb of the Earth's atmosphere. Detailed information about the measurement technique, the spectral bands observed and the target molecules can be found in the work of *Waters et al.* [2006]. MLS measurements of the middle stratosphere have a ~3–4 km (depending on the species) vertical resolution which becomes poorer (>6 km) in the upper stratosphere/lower mesosphere. The precision varies typically ranging from 0.03 ppm by volume (hereinafter ppmv) and 25 parts per billion by volume (hereinafter ppbv) at 100 hPa to 0.3 ppmv and 16 ppbv at ~1 hPa for O_3 and N_2O respectively [*Froidevaux et al.*, 2008; *Lambert et al.*, 2007]. The measurements of H_2O volume mixing ratio and temperature have a precision equal to 0.3 ppmv and 2.5 K respectively on the 100–0.1 hPa vertical range [*Lambert et al.*, 2007; *Schwartz et al.*, 2008]. The publicly available version 2.2 MLS measurements were used in this study. The data were filtered to select only measurements with values of status even, quality >1.0, convergence <1.5, and positive precision. These flags are provided in the "EOS MLS Level 2 data quality and description document" available for V2.2 [*Livesey et al.*, 2007].

[7] The MLS temperature measurements were used to provide interpolated data profiles on isentropic surfaces by fitting a spline function to the measurements. Along-track measurements on isentropic surface were then linearly interpolated onto a regular grid with an elementary square of 3°/3° resolution in longitude/latitude.

2.2. MIMOSA

[8] In order to perform MIMOSA simulations, we used the ERA-Interim reanalysis [*Dee et al.*, 2011] from the ECMWF model. ERA-Interim is the latest ECMWF reanalysis which is based on version Cy31r2 of the model with a spectral truncation of T255L corresponding to a resolution of 0.7° in latitude and longitude. ERA-Interim fields are provided over the whole period from 1989 to the present onto 37 pressure levels from 1000 hPa to 1 hPa or 60 model levels from 1000 hPa to 0.1 hPa. For this study, we used the ERA-Interim 37 pressure level outputs with a vertical resolution of 3 km approximately in the stratosphere. More details on ERA-Interim reanalysis are available in the paper of *Dee et al.* [2011].

[9] Potential vorticity (PV) maps have been calculated using the MIMOSA contour advection model [*Hauchecorne et al.*, 2002]. This model performs high resolution advection calculations based on the ECMWF analyzed wind, pressure and temperature fields to provide PV fields on isentropic surfaces. MIMOSA initially computes the PV field using the ERA- Interim analysis at a resolution of 1.125° in latitude and longitude (T106) which is vertically interpolated on an isentropic surface. This field is then interpolated on the original x-y grid centered on the North Pole with a horizontal resolution of 37 × 37 km (three grid points/degree) and advected with a time step of one hour.

[10] To preserve the homogeneity of the field, a regridding of the PV field on the original grid is made every 6 h. The information on diabatic changes in the PV field at large scales can be extracted from the ERA-Interim fields. In the MIMOSA model this is done by applying to the advected field a relaxation toward the ERA-Interim PV field calculations every ten days. This technique allows MIMOSA to run continuously over periods of several months in order to follow the evolution of dynamical barriers and fine scale structures such as vortex remnants and tropical intrusions [*Orsolini*, 2001; *Marchand et al.*, 2003; *Huret et al.*, 2006].

[11] A series of ten runs has been performed with the MIMOSA model at the 850 K (~31 km, ~10 hPa) isentropic surface for the whole period 2000–2009. A long-time run of eight months starting the 1st January has been performed for every year. The results obtained in this way have been used to investigate in detail the dynamical conditions associated with FrIAC and tropical intrusion events occurring in winter

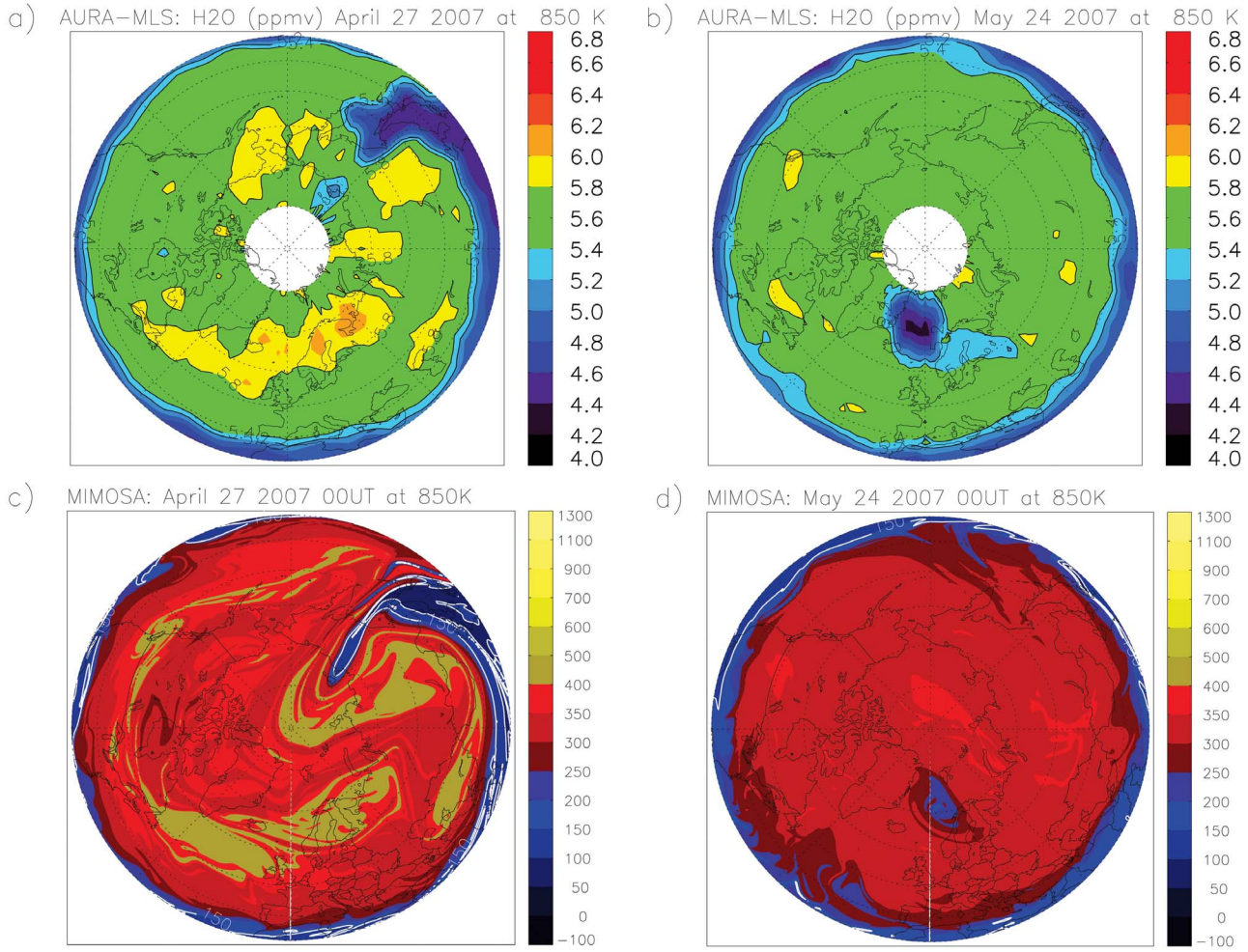

Figure 1. (a, b) Isocontours of water vapor mixing ratio (ppmv) from the MLS instrument interpolated on the 850K isentropic surface and (c, d) potential vorticity maps simulated by MIMOSA model. Figures 1a and 1c show 27 April 2007 during the intrusion leading to the FrIAC. Figures 1b and 1d show 24 May 2007 when the FrIAC is trapped at high latitudes. In Figure 1 and in remaining figures, potential vorticity is plotted in pvu (10^{-6} km^2 kg^{-1} s^{-1}).

and spring. In addition, zonal wind, meridional wind and temperature fields from the ERA-Interim reanalysis have been used to establish a climatology of the Northern Hemisphere heat fluxes and zonal wind conditions over the last decade. This climatology allowed us to improve the overall understanding of dynamical conditions responsible of FrIAC occurrences.

3. Recent FrIAC Episodes

[12] MIMOSA simulations and satellite measurements from MLS over the years 2005 to 2009 have been used to study FrIAC events. During this period a new case has been highlighted during spring 2007.

3.1. The New FrIAC Event on 2007

[13] Figure 1 shows a polar projection of the H_2O mixing ratio from the MLS measurements during the first stage of this FrIAC event (27 April 2007, Figure 1a), when the tropical intrusion was under development, and at a later stage when the tropical air mass was circling around the polar region (the 24 May 2007, Figure 1b). At the latter stage, the FrIAC was a well defined dynamical structure relatively isolated from the surrounding air. It was trapped in the easterly circulation above 70°N north, and persisted until the beginning of July 2007. We have compared the 850K isentropic surface H_2O mixing ratio measurements from the MLS instrument to PV maps from the MIMOSA model. Comparisons of the H_2O mixing ratio and the PV fields lead us to accept the MIMOSA model as a valid means of representing the evolution of this structure.

[14] Table 1 summarizes the main characteristic of this 2007 event, as well as the 2005 event described by *Manney et al.* [2006b] and the 2003 event [*Lahoz et al.*, 2007]. The duration of the 2003 event was roughly of one and a half months whereas the 2007 event lasted more than 2 months, and the 2005 event more than four months. These FrIAC lifetimes are based on tracer measurements. We report also typical values of potential vorticity on the 850K surface in the core of the FrIAC and in the surrounding air while

Table 1. Main Characteristics of 2003, 2005 and 2007 FrIAC Events

	2003	2005	2007
Intrusion	April 15th	March 27th	April 27th
End	Late May	Mid August	Early July
PV (pvu), Minimum in the FrIAC	150	54	80
PV (pvu), Surrounding the FrIAC	350	370	350
References	*Lahoz et al.* [2007]	*Manney et al.* [2006b]	This paper

FrIACs remained in the polar region. For the 2005 and 2007 events the characteristic values of PV are quite similar for the core of the FrIAC as well as for the surrounding air masses. The 2003 event appears to have been the least intense as its minimum in PV was the shallowest and its duration the shortest (Table 1). This relatively lower PV value suggests an intrusion originating from the border between the subtropics and midlatitudes in the Northern Hemisphere which consequently persisted only for a few weeks.

[15] A comparison of the 2005 and 2007 FrIAC trajectories when they were located at latitudes higher than 60°N is shown in Figure 2. Their location can be followed based on the location of the maximum value of the N_2O mixing ratio in the core of the FrIAC at 10 hPa. The 2007 event from 28 April to 30 June was located approximately at 70°N, with four rotations occurring during two months before it disappeared. For the 2005 event the trajectory of the FrIAC core was more northward at approximately 70–80°N, with seven rotations around the pole occurring during four and a half months. From the tropical intrusion (29 March 2005) to mid-April, the FrIAC was in its "spin-up phase" [*Allen et al.*, 2011] associated with the period before the shift from winter westerlies to summer easterlies that occurred during the final stratospheric warming (FSW). The FrIAC was then advected by westerlies (until 13 April 2005) before it was trapped in the easterly regime. This phase did not occur for the FrIAC event in 2007, which was directly advected by the summer easterlies after its intrusion.

[16] To investigate the vertical structure of both FrIAC events (2005 and 2007) we have selected the vertical profiles of N_2O, H_2O and O_3 within FrIAC cores as they circle around the globe. The criterion applied to select the points was based on the maximum value of the N_2O mixing ratio at each MLS level 100.0, 68.1, 46.4, 31.6, 21.5, 14.5, 10.0, 6.8 and 4.6 hPa northward of 60°N. Then we could follow the vertical evolution of the different species in Figure 3 as a function of time along the FrIAC tracks. The N_2O 140 ppbv and 180 ppbv isocontours are marked by the black solid and dashed lines respectively. The vertical extent of both episodes in their initial stages is similar extending over the [21.5–7] hPa pressure range in 2007 (Figures 3a, 3b, and 3c) and the [21.5–5] hPa pressure range in 2005 (Figures 3d, 3e, and 3f). Although the FrIAC signatures seem extended down to 21.5 hPa in the Figure 3, we have chosen this limit which corresponds to the lowest MLS level where the FrIACs are detected. Below this limit, the selected points depict the maximum of N_2O northward of 60°N which do not correspond to the FrIAC anomalies.

[17] The vertical N_2O profiles (Figures 3a and 3d) reveal a similar behavior of both FrIACs with altitude. The vertical extent of the FrIACs appears to decrease with time while keeping their strongest signature at 10 hPa and 14 hPa in 2007 and 2005 respectively depicted by the 180 N_2O ppbv isocontours. In their recent paper, *Allen et al.* [2011] highlight two dynamical phases of the evolution of the 2005 FrIAC following the "spin-up phase." During the "anticyclonic phase," the FrIAC is trapped in the developing summer easterlies (April–May) and seems resistant to the weak vertical wind shear. In late May, the dynamical signature of the anticyclone decays due to diabatic processes exposing the tracer anomaly to the horizontal and vertical wind shear during the "shearing phase." This late phase is characterized by the vertical tilt of the FrIAC. The "shearing

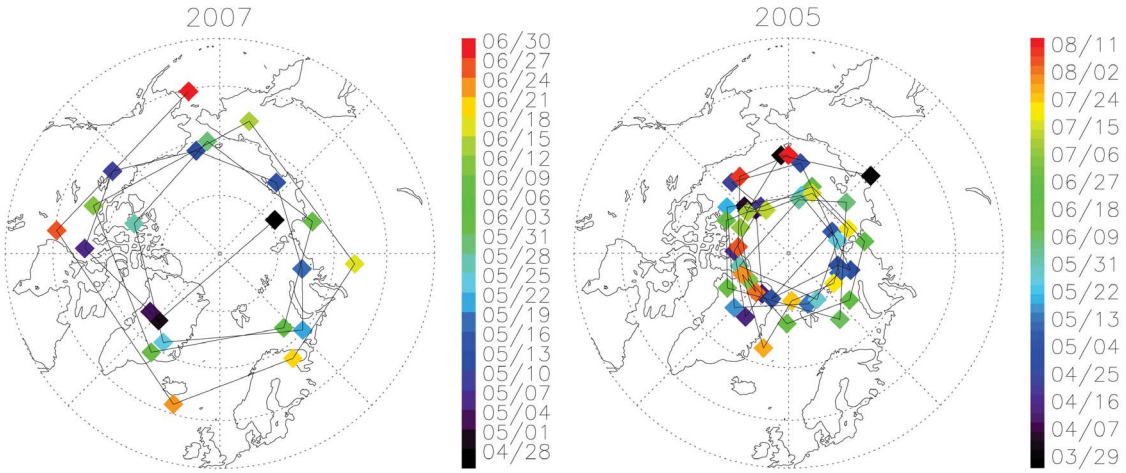

Figure 2. Paths of the core of FrIACs in (left) 2007 and (right) 2005 at 10 hPa. The FrIAC core is where the maximum value of the N_2O mixing ratio is located, based on EOS-MLS observations. The color code corresponds to the dates (format MM/DD) associated with the FrIAC locations. Black (red) square corresponds to the start (finish) of the FrIAC trajectories, respectively.

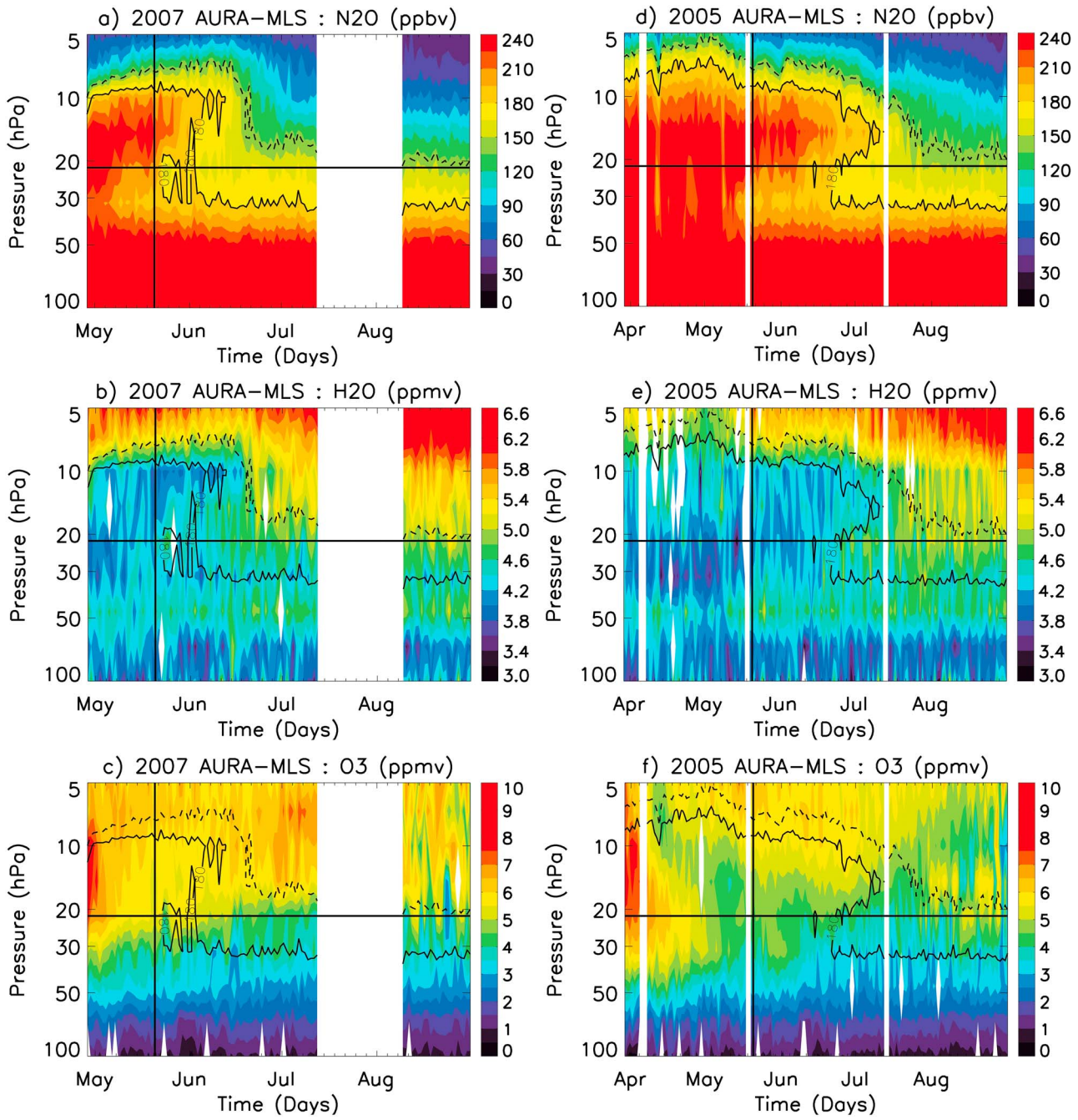

Figure 3. Time evolution of vertical profiles of N_2O, H_2O and O_3 volume mixing ratios inside the FrIAC cores in (a, b, c) 2007 and (d, e, f) 2005 obtained from the AURA-MLS instrument. The daily vertical profiles were selected using the criterion of maximum mixing ratio of N_2O northward of 60 N for each MLS pressure level in the range [100–5] hPa. The black and dashed isocontours displayed on each figure correspond to 180 ppbv and 140 ppbv N_2O respectively. The vertical black solid line corresponds to the transition between the "anticyclonic phase" and the "shearing phase," in 2007 and 2005. The horizontal black solid line depicts the lowest MLS level where the FrIACs have been detected (21.5 hPa). White areas indicate a lack of data.

phase," corresponding to the period after the vertical solid line (Figures 3a and 3d), appears in the N_2O isocontours as a progressive decrease in the vertical extent from 21.5 hPa in late May to 10 hPa (2007) and 14 hPa (2005). In 2007, the tropical intrusion leading to the FrIAC occurred one month later than in 2005. As a consequence, the "anticyclonic phase," corresponding to the period before the vertical solid line (Figure 3a), was shorter ending in late May as it did in 2005 (Figure 3d). The close timing of transition between the "anticyclonic phase" and the "shearing phase" support the

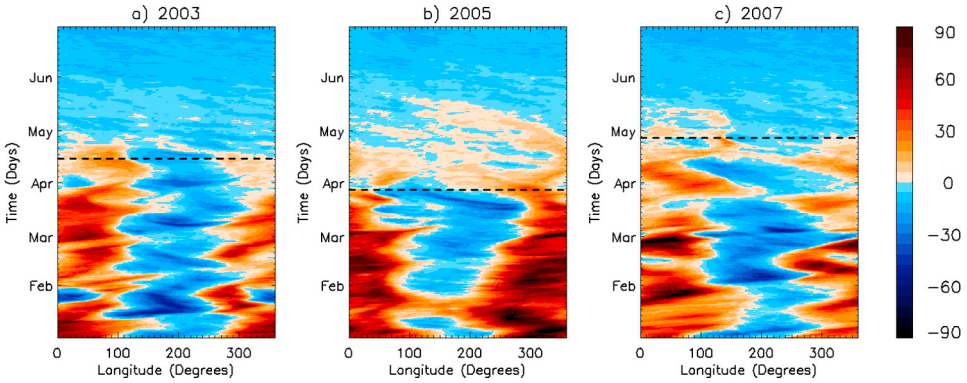

Figure 4. Hovmöller diagrams (longitude VS time) of zonal wind fields at 49.5°N from ERA-Interim reanalysis interpolated on the 850K isentropic surface for (a) 2003, (b) 2005 and (c) 2007. The color code ranges from dark blue (strong easterlies) to dark red (strong westerlies). The black dashed line corresponds to the FrIAC intrusion date.

dynamical arguments put forward by *Allen et al.* [2011] about the timescales of radiative damping.

[18] However, the duration of the "shearing phase" is very different between the two cases. Examination of the persistence of the N_2O and H_2O anomalies reveals that the "shearing phase" lasted one and an half months longer in 2005 than in 2007. Several additional investigations would be needed to improve our understanding of such variability. In particular, it would be interesting to investigate in more detail the link between the tilt of the FrIAC caused by the wind shear and the associated mixing processes.

[19] Both the 140 ppbv and 180 ppbv N_2O isocontours have been overlaid on the H_2O and O_3 time evolution in the core of the FrIACs. The tropical low H_2O mixing ratio of 5 ppmv corresponds approximately to the 140 ppbv N_2O FrIAC signal (dashed isocontour). Note that for the 2005 case the H_2O 5 ppmv signal persisted until the end of August. The 4.2–4.4 ppmv H_2O mixing ratio signal corresponds to the 180 ppbv N_2O signal (black isocontour).

[20] Regarding O_3, the tropical high values observed of greater than 7 ppmv at the beginning of the FrIAC events disappear very quickly (in a few days) compared to N_2O and H_2O tracer signals. This high ozone mixing ratio signal in the FrIAC cases (Figures 3c and 3f) also appear in approximately the same range of pressure [21.5–7] hPa as for the passive tracers. Immediately after the FrIAC intrusions, the decrease in ozone mixing ratio is faster in the uppermost levels, near 10 hPa, than in the lowest ones where the ozone signal decreases slowly, near 20 hPa. This mean that the FrIAC ozone signal durations depend more on the gaseous chemistry and the photochemistry than on mixing processes seen mainly on FrIAC tracers signals during the "shearing phase" in late-May. Further modeling investigations would be necessary to improve our understanding of specific chemistry inside the core of the FrIACs.

3.2. Dynamical Conditions During FrIAC Recent Episodes (2003, 2005, 2007)

[21] Zonal wind Hovmöller diagrams interpolated on the 850K isentropic surface (Figure 4) show the dynamical evolution of the stratosphere at midlatitudes (49.5°N) from January to the end of July. The dashed black lines correspond to the FrIAC intrusion dates. During the three periods of interest, the midlatitudes were dominated by the ridge/trough pair Aleutian High/Polar Vortex (zonal wave number 1) respectively seen by the alternation between the easterly circulation of the Aleutian High (hereafter AH) in the [100°E–280°E] sector and the westerly circulation of the polar vortex in the [280°E–100°E] sector. The persistence of the AH and the polar vortex suggests that the wave activity was maintained during the whole January/May period, alternating in time between strong and weak amplitudes. During 2003 and 2005, the signature of the AH/Polar Vortex in the zonal wind fields was still present when the FrIAC intrusions occurred before decreasing and turning to the weak summer easterly circulation. This feature was weaker in 2007.

[22] Analysis of zonal winds and potential vorticity maps during the FrIAC intrusions reveal strong similarities as the Figure 5 suggests. MIMOSA PV isocontours and ERA-Interim zonal winds are shown at the 850 K isentropic surfaces when the tropical air mass reached the midlatitudes on the 13 April 2003 (Figures 5a and 5d), the 24 March 2005 (Figures 5b and 5e) and the 25 April 2007 (Figures 5c and 5f). Tropical/vortex air mass signatures have, respectively, low/high PV values represented in blue/yellow. At the time of the intrusions, the polar vortex had already broken up, following the onset of the final warming, and the associated remnants were spread over the Northern Hemisphere. The PV maps show episodes of Rossby waves breaking in the midlatitude "surf zone" [*McIntyre and Palmer*, 1983, 1984] when the tropical intrusions occurred, depicted by the inversion of the latitudinal PV gradient [*Baldwin and Holton*, 1988; *Hitchman and Huesmann*, 2007] located in the ranges [135°E–145°E, 40°N–60°N], [45°E–90°E, 25°N–60°N] and [135°E–170°E, 30°N–60°N] for the 2003 (Figure 5a), 2005 (Figure 5b) and 2007 (Figure 5c) cases respectively.

[23] In 2003 (Figure 5a), the vortex remnants with a PV value higher than 400 pvu were located over Eurasia and North Atlantic. Relatively low PV values were located mainly southward of 30°N and an anomaly of low PV can be seen centered on [180°E, 55°N] corresponding to tropical air masses trapped into the AH a few days earlier. The tropical air intrusion started to develop above east Africa, just

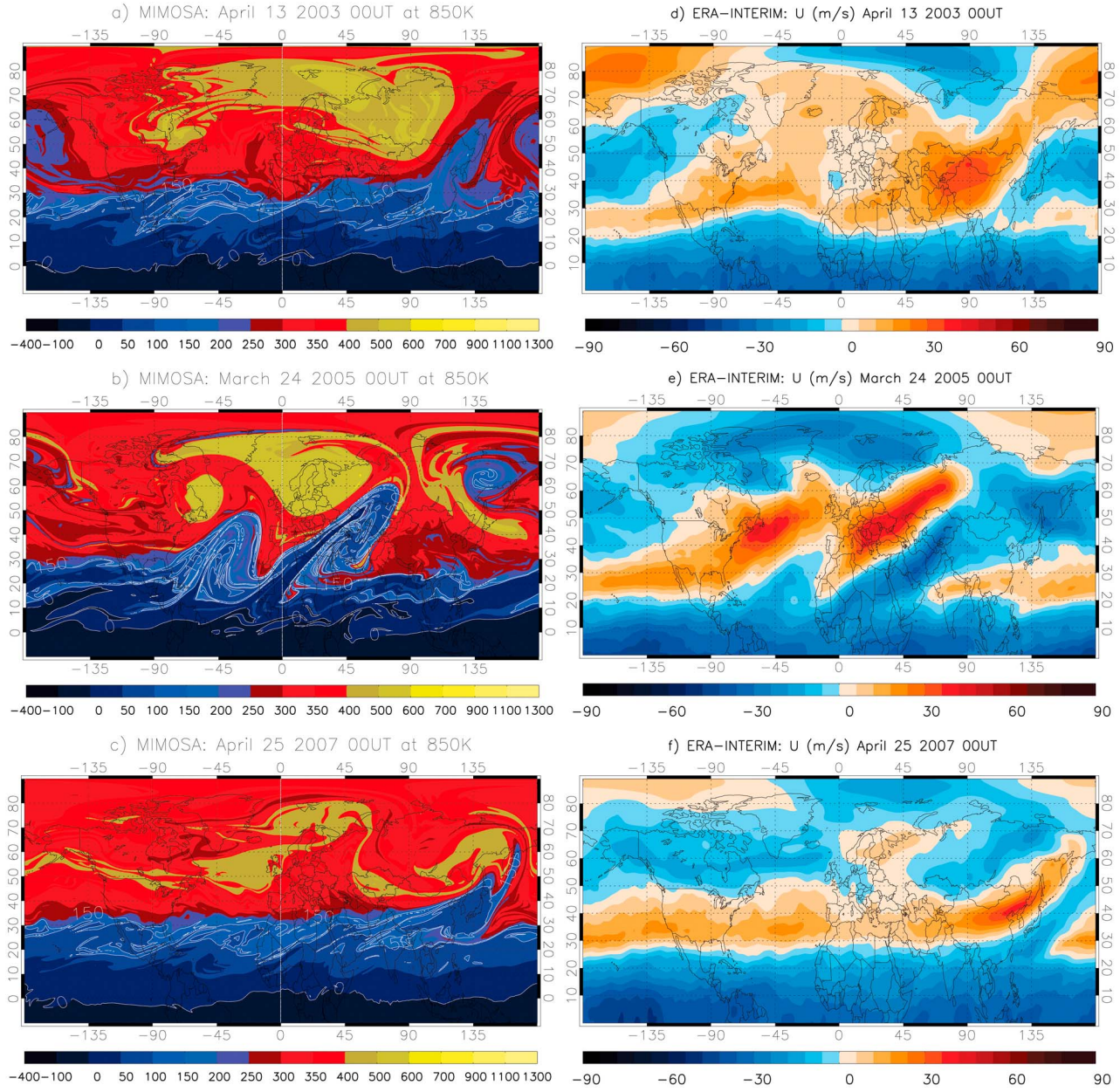

Figure 5. (a, b, c) Northern Hemisphere maps of PV isocontours calculated using the MIMOSA model and (d, e, f) zonal winds from the ERA-interim reanalysis during the FrIAC intrusions on the 850 K isentropic surface in (top) 2003, (middle) 2005 and (bottom) 2007.

southward of the main vortex remnant, and on April 13th is seen to have been advected to the North Pole between the polar vortex and the AH near 120°E at midlatitudes.

[24] The tropical intrusion in 2007 (Figure 5c) was similar to the 2003 event following the same trajectory and occurring approximately at the same time period. However, it can be seen that the vortex remnants were thinner and the residues of tropical air masses trapped into the AH did not appear. As occurred in the 2003 case, a stretched vortex remnant was located just Northward of the tropical intrusion [135°E, 40°N].

[25] In 2005, an early and strong final stratospheric warming [*Manney et al.*, 2006a] occurred in mid-March (see section 4.1). This warming was characterized by the displacement of the polar vortex toward midlatitudes, and was followed by a deep tropical intrusion trapped at polar latitudes and the break up of the polar vortex. The anticyclone corresponding to the intrusion is located at 135°E and 65°N in the PV map of the 24 March (Figure 5b). At the same time, two deep tropical intrusions developed at midlatitudes southward of the main vortex remnants. The intrusion starting above Africa merged with the anticyclone already present leading to the FrIAC development. The other tropical intrusion, above the Atlantic Ocean, remained confined at midlatitudes before dispersing a few days later.

[26] Comparison with the Hovmöller diagrams of zonal winds at 49.5°N (Figure 4) shows that the zero zonal wind lines oscillating around 100°E correspond roughly to the

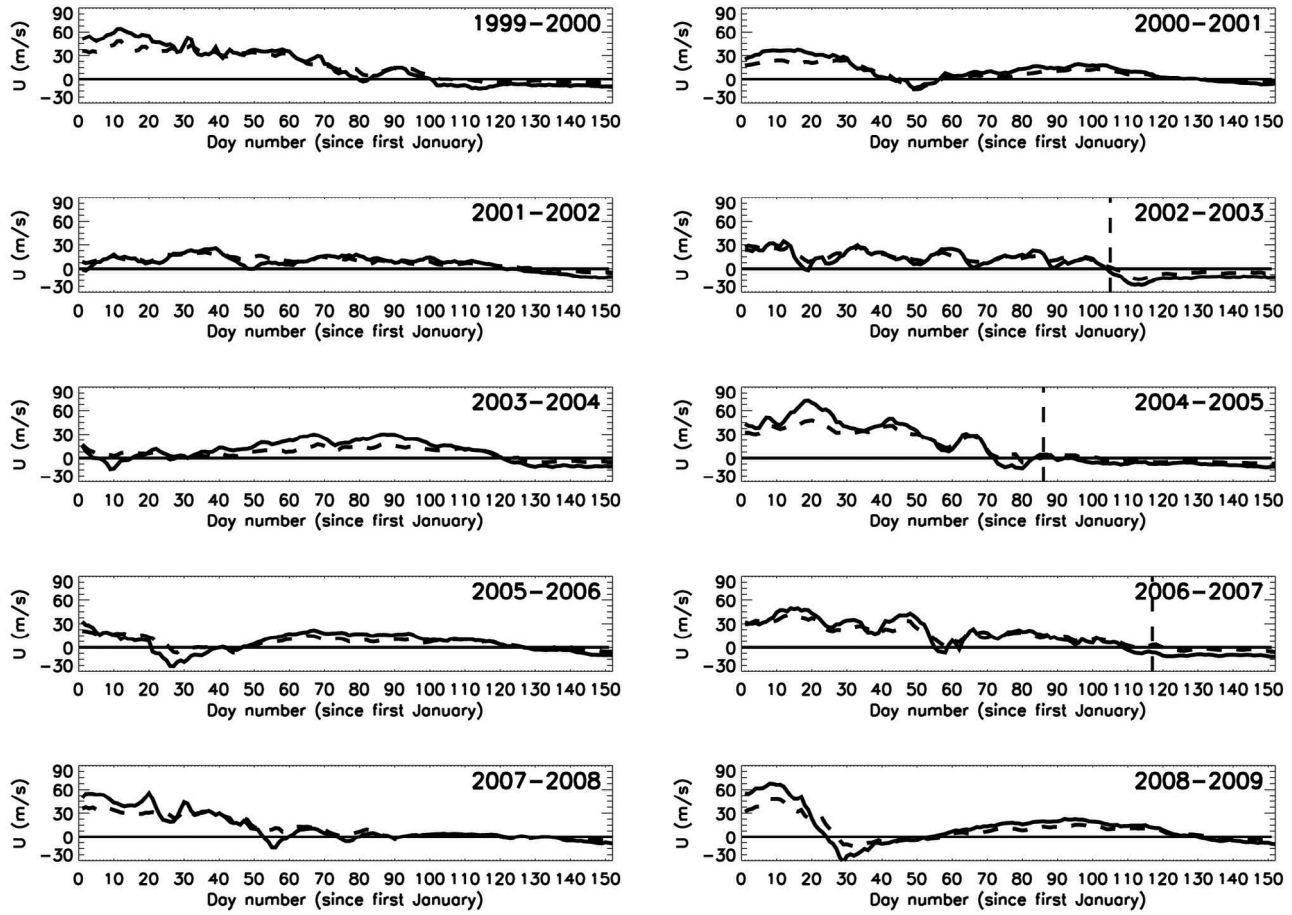

Figure 6. Zonal-mean zonal wind from ERA-interim reanalysis at 60°N and 10 hPa (solid black line) and 30 hPa (dashed black line) during the period January/May periods from 2000 to 2009. The vertical black dashed lines correspond to the FrIAC intrusion dates.

tropical intrusion locations seen in PV maps at midlatitudes (Figure 5). This region has been previously identified by *Harvey and Hitchman* [1996] as the preferred location for exchanges from the subtropics to the extratropics at the west edge of the AH. The PV maps also reveal that the southward displacement of the vortex remnants at midlatitudes seems to be a necessary condition leading to the growth of the tropical intrusion located just southward.

[27] The zonal circulation can be divided into three separated regions (Figures 5d, 5e, and 5f). The inter-tropical zone which, in each case, was driven by the easterly phase of the quasi-biennial oscillation from 0° to 30°N; the midlatitude "belt" from 30°N to 55°N dominated by a westerly flow that has been previously reported by *Waugh* [1996] as a necessary condition for intrusion toward the pole; and the polar region which started to reverse toward the easterly summer regime. The meridional gradient of zonal wind between tropical and midlatitudes was strong, suggesting a region of intense horizontal shearing. In the region where the vortex remnants were mainly located, a strong cyclonic cell appeared a few days before the tropical intrusion. During the growth of the intrusion southward of the remnants, an anticyclonic cell developed, with the zero zonal wind line centered on the trajectory of the tropical intrusion. Comparing this cell between the 2003, 2005 and 2007 events shows that the intensity of the tropical intrusion seems to depend on the horizontal zonal wind shear. The stronger the anticyclonic cell, and the more intense the shearing, the more likely is tropical air to be transported poleward from low latitudes.

[28] After having characterized the dynamical conditions during several observed FrIAC events, we investigate in more details the entire last decade to understand why such events do or do not develop.

4. Climatological Occurrences of FrIACs: The Role of Stratospheric Warmings and the Quasi-Biennial Oscillation

4.1. Link With Major Sudden Stratospheric Warmings

[29] Major sudden stratospheric warmings (SSWs) occur when the zonal westerly circulation at 60°N and 10 hPa reverses to easterly (WMO, 2007). The evolution of the mean zonal winds at 60°N and 10 hPa (30 hPa), solid (dashed) line respectively, are shown in Figure 6 for the last decade. The FrIAC intrusion dates are again indicated by the vertical black dashed line. Three cases of SSW appeared during the following northern winters: 2000–2001 (Julian days 45 to 55), 2005–2006 (Julian days 20 to 37) and 2008–

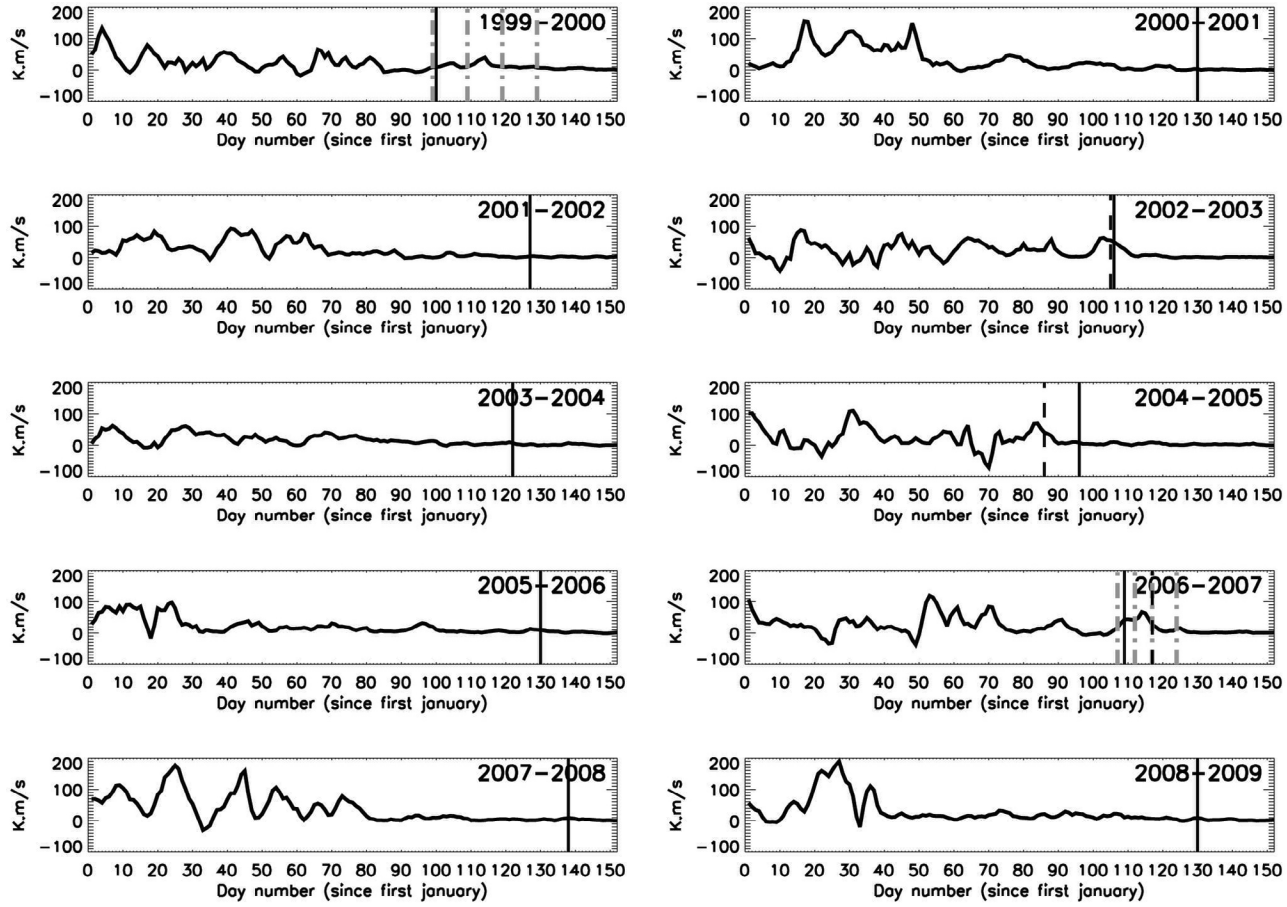

Figure 7. Zonal-mean meridional eddy heat flux (in k m s^{-1}) averaged on the latitude band [45,55]°N at 30 hPa calculated from ERA-Interim reanalysis during the January–May periods from 2000 to 2009. Black solid (dashed) lines correspond to the reversal of the zonal-mean zonal wind to easterlies at 10hPa (FrIAC intrusion). Grey dashed-dotted lines correspond to the dates of the maps in Figures 8a, 8b, 8c, and 8d (2007) and Figures 9a, 9b, 9c, and 9d (2000).

2009 (Julian days 23 to 50). They are also characterized by the temporary reversal of the zonal circulation from westerlies to easterlies at 30 hPa, underlying the strong intensity of the SSW. They were then followed by the recovery of a weak undisturbed polar vortex. During the 2001–2002 and 2003–2004 winters, an early SSW occurs before the Julian day 0 and at the Julian days 4 to 14 respectively. The 2007–2008 winter shows a strong westerly circulation weakened by a late SSW (Julian days 52 to 60), which prevented the recovery of the vortex. The winters described previously (2000–2001, 2001–2002, 2003–2004, 2005–2006, 2007–2008 and 2008–2009) are characterized by a slow transition to summer easterlies during a late final warming which occurred in early May (after Julian day 120).

[30] On the other hand, the 1999–2000, 2002–2003, 2004–2005 and 2006–2007 winters show common features, with a strong and disturbed polar vortex which decreased progressively until an abrupt and early final warming occurred in mid-April (Julian day 105). In 2003, the first SSW occurred about day 18 characterized by the displacement of the polar vortex along the Greenwich meridian through midlatitudes. The polar vortex was then subject to strong oscillations between the mid and polar latitudes due to the propagation of planetary waves (seen on MIMOSA outputs but not shown here). This is suggested by the intense fluctuations of the zonal mean zonal winds that occurred at 10 hPa and 60°N (Figure 6). However, the polar westerlies were maintained until the final warming when the FrIAC was pulled to polar latitudes. In 2005, a strong stratospheric warming occurred during the late winter/early spring, allowing the FrIAC intrusion. This strong SSW can be considered as a kind of precursor to the final warming which took place ten days later.

[31] In 2007, the polar night jet was weakened by a short SSW (Julian days 55 to 58) characterized by the displacement of the polar vortex over Northern Europe. In this case, the MIMOSA PV maps show that the vortex was not destroyed, allowing it to maintain high PV values as was the case in 2003.

[32] The propagation of planetary waves is investigated using the meridional eddy heat fluxes $\langle\, v'T' \,\rangle$ over the last decade at 30 hPa, and averaged over the [45°N–55°N] latitude band (Figure 7). The link with the zonal-mean zonal winds at 10 hPa and 60°N (Figure 6) shows that following the deep SSWs during the 2000–2001, 2005–2006 and 2008–2009 winters, when the polar vortex recovered, the

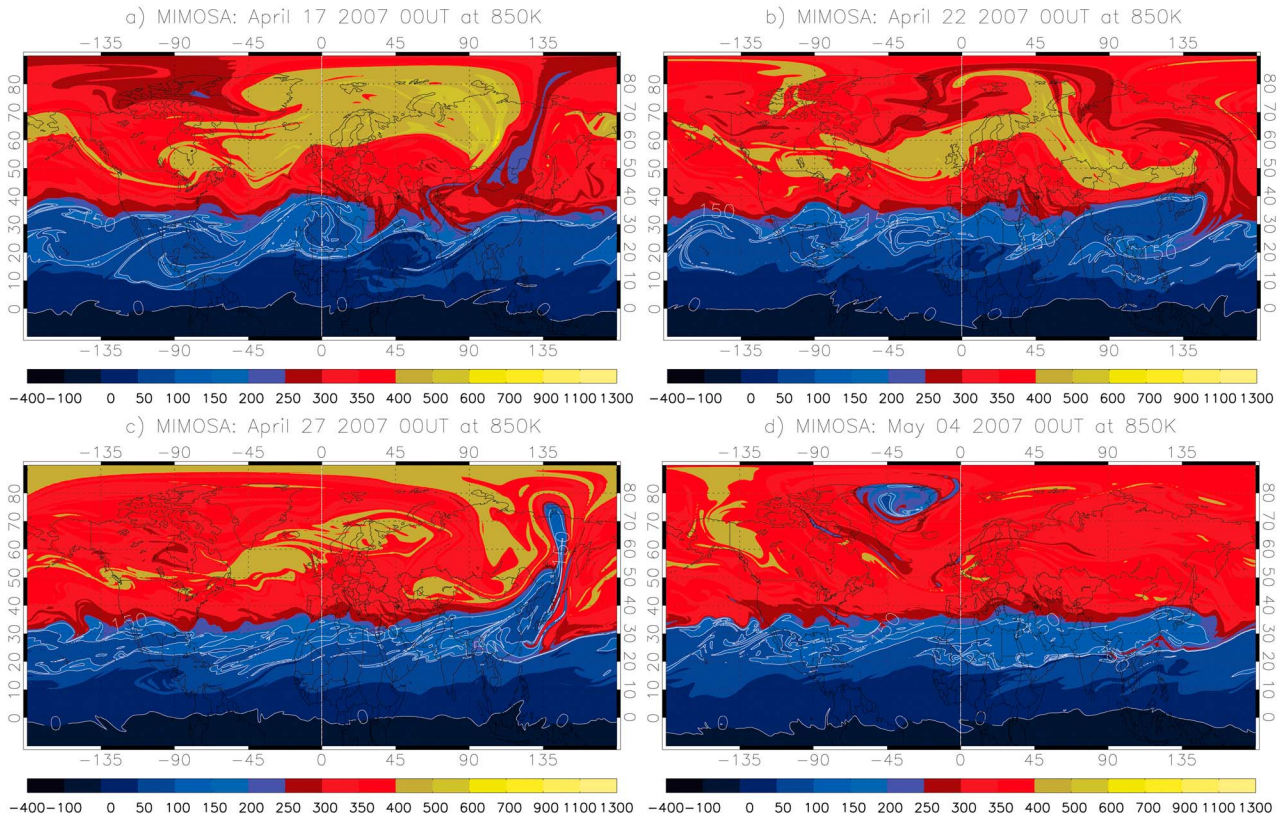

Figure 8. PV maps calculated using the MIMOSA model on the 850 K isentropic surface for spring 2007. Four dates are shown: (a) April 17th, (b) April 22nd, (c) April 27th and (d) May 4th 2007.

upward propagation of Rossby waves was inhibited after the Julian days 50, 30 and 40 respectively (Figure 7).

[33] Figure 6 shows that the 2001–2002, 2003–2004 and 2007–2008 winters are characterized by a weak and undisturbed polar night jet following the SSWs which occur around the Julian days 0, 10 and 55 respectively. In these years, first the decrease then the suppression of the upward heat flux occurs approximately 50 days before the final warming. Very weak heat fluxes during the final warming prevent the intrusion of tropical air masses.

[34] The years that include FrIACs events exhibit similar behavior in the heat flux. The planetary wave propagation is maintained during the entire period from January to the final warming, when a peak in heat flux is seen. These results are in good agreement with those depicted by the zonal wind's Hovmöller diagrams (Figure 4). The FrIAC intrusion occurs, in each case, soon after the last peak in the heat flux, suggesting sufficient wave activity to allow the tropical air mass to move toward the polar latitudes.

[35] During the last decade, several cases of major SSWs have been reported: in February 2001 [*Jacobi et al.*, 2003], January 2004 [*Manney et al.*, 2005; *Liu et al.*, 2009], January 2006 [*Manney et al.*, 2009], February 2008 [*Coy et al.*, 2009] and January 2009 [*Manney et al.*, 2009]. In particular, the last three cases have been studied by *Orsolini et al.* [2010] using the GOES-5 analysis. These latter shown that the shifting of the zonal wind phase to easterly during the SSW propagates downward and then removes the critical line, where the zonal mean zonal winds is equal to zero, in the lower stratospheric layers. This leads to the inhibition of the upward propagation of planetary waves [*Tomikawa*, 2010] which play a crucial role on the mechanisms that operate during FrIAC events. The three cases of FrIACs recorded during the last decade show similar winter dynamical conditions, viz. absence of a major SSW and preservation of planetary wave activity until the FSW. In spite of these propitious conditions during the 1999–2000 winter, a FrIAC intrusion did not occur. We now propose to investigate in detail for 2006–2007 the necessary conditions for a FrIAC event to occur and to compare them to the conditions in 1999–2000 around the period of the FSW.

4.2. Comparison of 2007 and 2000 Conditions

[36] Four stages of the final warming between the 17 April and 4 May 2007 identified using 850K PV maps are shown Figure 8 with the associated ERA-Interim zonal mean eddy heat fluxes at 30 hPa in the [45°N–55°N] latitude range in 2006–2007 (Figure 7). The gray vertical dashed-dotted lines in Figure 7 correspond to the dates of the four stages (Figure 8) and the vertical solid line depicts the date of the final warming as before.

[37] On the 17 April 2007 (Figure 8a), the polar vortex (in green/yellow) started to be irreversibly distorted into thin filaments spreading at midlatitudes over North America and North East Asia. At this stage, the heat flux in 2006–2007 (Julian day 107, Figure 7) started to increase sharply leading to the weakening of the polar vortex.

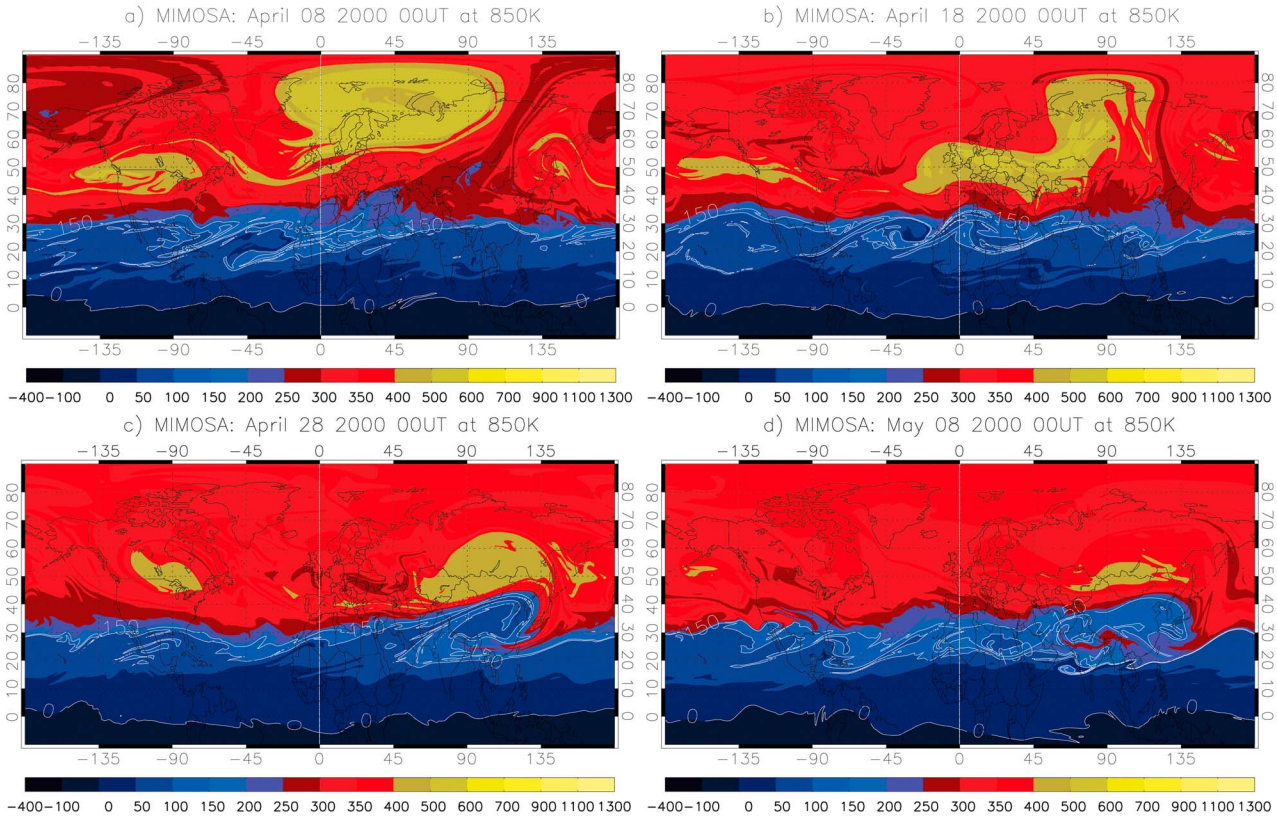

Figure 9. PV maps calculated using the MIMOSA model on 850 K isentropic surface for spring 2000. Four dates are shown: (a) April 8th, (b) April 18th, (c) April 28th and (d) May 8th 2000.

[38] By the 22 April 2007 (Figure 8b), the polar vortex had been displaced toward midlatitudes, and it then broke up into high PV remnants due to the strong planetary wave activity. The associated heat flux (Julian day 112, Figure 7) increased to 40 k m s^{-1}. A high PV remnant which included a strong cyclonic cell (not shown) was located above Mongolia. Midlatitude planetary-wave breaking began in the weak zonal wind region (southward of the "westerly belt"), depicted by the meridional PV gradient inversion located around [30°N; 135°E] (Figure 8b). It allowed the advection of a tropical air mass (low PV) southward of the vortex remnants to form the dipolar PV cell centered around [120°E, 40°N].

[39] On the 27 April 2007 (Figure 8c), the tropical intrusion quickly advected to polar latitudes in a thin filament along with the northward vortex remnants over the pole. At this date, the heat flux sharply decreased characterizing the end of the winter planetary wave episode. Two days earlier, the heat flux in 2006–2007 (Figure 7) reached its maximum higher than 60 k m s^{-1}, which correlated with the onset of the tropical intrusion (Figure 5c) toward polar latitudes by the 25 April 2007.

[40] By the 4 May 2007 (Figure 8d), the FrIAC was located at polar latitudes and advected with the summer easterlies; the high PV vortex remnants had dissipated and the heat flux increased a final time before falling to 0 k m s^{-1}, thus showing that planetary waves could not propagate further in the summer easterlies.

[41] In order to improve our understanding of the mechanisms behind the FrIAC formation, northern spring 2000 has been investigated in the same way (Figures 9 and 7). On the 8 April, 2000 (Figure 9a), the polar vortex was located over Northern Europe and started to be weakened by erosion into thin filaments advected at midlatitudes. These PV contours are similar to the first map (Figure 8a) of the 2006–2007 event. At the same time, the heat flux started to increase. Before the 18 April 2000 (Figure 9b) the vortex had been displaced to midlatitudes corresponding to the first peak in the heat flux at the Julian day 105 (1999–2000, Figure 7) and was then distorted into a major remnant located over Europe and West Asia.

[42] Five days later, when the maximum in heat flux was reached (1999–2000, Figure 7), the remnant was separated into two lobes and a wave breaking event started (not shown). Then a lobe is advected over North America, while the other remained over the Himalayan Chain (Figure 9c) while a precursor of tropical intrusion developed southward forming the dipolar PV cell.

[43] On the 28 April 2000, following the wave breaking event, the heat flux (1999–2000, Figure 7), has decreased sharply. By the 8th of May, 2000 (Figure 9d), the stationary dipolar cell had considerably weakened, as seen in the decrease of the remnant area and the PV value as well as the intensity of the tropical air mass vorticity.

[44] The detailed comparison between these two cases enables us to establish the dynamical conditions and the chronology needed for the FrIAC intrusions. The planetary waves drive the tropical intrusion mechanisms as we have shown previously. If the wave activity still persists until the

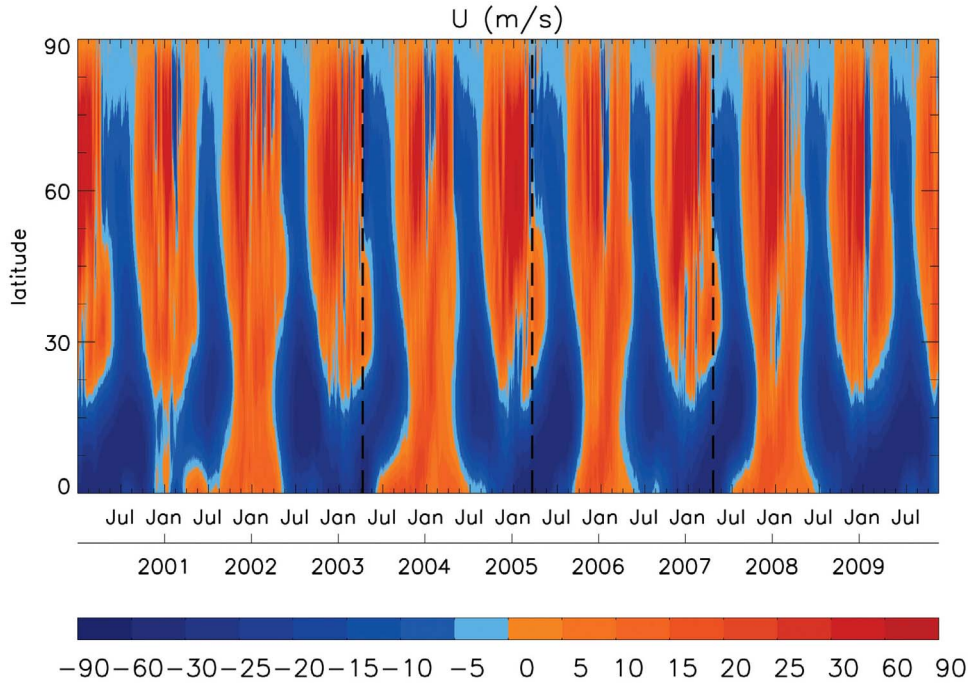

Figure 10. Zonal mean of the zonal wind from ERA-Interim reanalysis at 10 hPa as a function of time from January 2000 to January 2010 over the 0°N–90°N latitude range. Red color corresponds to westerly circulation and blue color to easterly circulation. The vertical black dashed line corresponds to the FrIAC intrusion dates.

final warming, then the FrIAC events can be initiated. The polar vortex, which starts to weaken, is displaced toward midlatitudes driven by the wave propagation. At this stage, the vortex breaks up into remnants of high PV values and leads to a strong horizontal shearing between the remnant westerlies and the tropical zonal flow. This favors the formation of a dipolar PV cell arising from the association of vortex remnants (poleward) trapped in a cyclonic circulation and a tropical air mass (equatorward) trapped in an anticyclonic circulation. Wave breaking events then occur in the vicinity of the anticyclone to homogenize the PV gradient. Such episodes inhibit the upward propagation of planetary waves as diagnosed in the heat flux fields. Subsequently, if the wave breaking is sufficiently strong, the tropical air mass is pulled poleward during the wave breaking episode as occurred for the 2006–2007 case, or else the dipolar cell persists a few days before finally weakening as occurred in the 1999–2000 case. Moreover, the zonal mean zonal wind and associated heat flux in 2000 (Figures 6 and 7) allow us to identify a short SSW around the Julian day 80 which is followed by the decrease of the heat flux before the onset of the FSW. This suggests that the late SSW during the spring 1999–2000 could be partly responsible for the weak wave activity preventing any tropical intrusion.

4.3. Is There a Link Between FrIACs and the Quasi-Biennial Oscillation Phase?

[45] The QBO plays a major role in the dynamical evolution of the middle stratosphere [*Baldwin et al.*, 2001]. Several studies have been undertaken to establish a link between the phase of the QBO and its influence on the Northern polar stratosphere. Based on a statistical study of the 1962–1977 period, *Holton and Tan* [1980, 1982] pointed out the fact that the easterly phase of the QBO could facilitate the occurrence of a major SSW. They showed that during the easterly phase of the QBO, the stratospheric polar vortex is weaker, warmer, and more disturbed. They suggested that the QBO phase in the tropics modulates the effectiveness of the waveguide for the midlatitude planetary waves that propagate through the winter stratosphere. The Holton and Tan relationship (HT hereafter) has been since re-examined by several observational and modeling statistical studies that included external factors such as the solar activity or the influence of the upper stratosphere [*Naito and Hirota*, 1997; *Gray et al.*, 2004; *Lu et al.*, 2008; *Naoe and Shibata*, 2010]. It seems to be now generally assumed that the HT relationship between the temperature of the polar vortex and the QBO phase is verified. However, diagnostic analysis of the Eliassen-Palm flux does not show more poleward propagation in the midlatitude stratosphere as the HT mechanism suggests.

[46] The mean zonal wind at 10 hPa of the last decade from the equator to the North Pole is represented in Figure 10. The latitude band between 0°N and 25°N is driven by the QBO which is, at 10 hPa, in the westerly phase during the 2001–2002, 2003–2004, 2005–2006 and 2007–2008 winters and in the easterly phase during 1999–2000, 2002–2003, 2004–2005, 2006–2007 and 2008–2009 winters. For the 2000–2001 winter, the phase of the QBO at 10 hPa is not clearly defined.

[47] Northward of 25°N, the behavior of the zonally averaged zonal wind depicts the alternation between the eastward dynamical regime of the winter (polar vortex) stratosphere and the summer (anticyclone) stratosphere associated with easterlies. The major SSWs of 2000–2001,

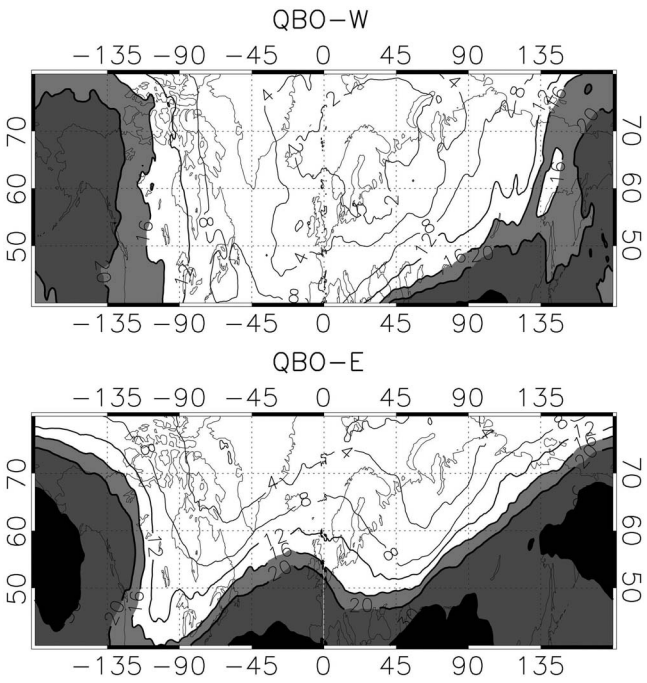

Figure 11. Frequency of occurrence (in percent) of air mass with PV lower than the zonal-mean PV at 30°N and 850 K during January/February for the QBO westerly phase (years 2002, 2004, 2006, 2008) on the top and the QBO easterly phase (years 2000, 2003, 2005, 2007, 2009) on bottom. Dark contours are for frequencies higher than 16%.

2003–2004, 2005–2006 and 2008–2009 winters are characterized by a robust reversal of the zonal circulation northward of 60N for several weeks. Figure 10 shows that three of the four observed major SSWs occur under the westerly phase (2003–2004; 2005–2006) or during the transition phase (2001–2002) of the QBO which is not in good agreement with the HT statistical relationship but similar to the results of *Lu et al.* [2008], although we consider here only 10 years of data.

[48] The intrusions associated with FrIACs (vertical dashed line in Figure 10) in 2003, 2005 and 2007 occurred when the QBO was easterly in the [50–3] hPa, [40–1.5] hPa and [40–3] hPa ranges respectively, and, as seen previously, no deep SSW occurred during winter. The 1981–1982 and 1993–1994 FrIAC cases pointed out by *Manney et al.* [2006b] were accompanied by an easterly circulation at the tropics in the [100–5] hPa and [50–2] hPa ranges respectively. Hence, the five winters corresponding to known FrIAC events are characterized by an easterly QBO phase around 10 hPa.

[49] In addition, we have considered the occurrences of tropical intrusions during the last decade under both the easterly phase of the QBO (QBO-E) and the westerly phase of the QBO (QBO-W), and for the January/February (Figure 11) and March/April (Figure 12) periods. Using MIMOSA PV calculations, we have considered the frequency of occurrence (in percent) defined by PV values lower than the daily zonal mean PV at 30°N computed with MIMOSA results. The 2000–2001 winter was not taken into account because the QBO phase was undefined (Figure 10).

[50] The frequency of intrusions during the January/February period (Figure 11) shows that most tropical intrusions occur at the location of the AH anticyclone for both, QBO-W (top) and QBO-E (bottom) with a frequency higher than 20%. The minimum of tropical intrusion frequencies corresponds to the statistical main location of the polar vortex [*Harvey et al.*, 2002]. A secondary maximum corresponding to zonal wave number 2 was recorded over the Atlantic Ocean and corresponds to the region where intrusions occur under QBO-E conditions rather than QBO-W conditions. The maximum frequency of tropical intrusions reaches higher values (30%) for the QBO-E case than for the QBO-W case (20%). This suggests that the AH is extended more poleward and the vortex more equatorward along the prime meridian (top) under the QBO-W. Figure 11 suggests that during the January/February months over the last decade and under an easterly QBO, the number of tropical intrusions is higher than under a westerly QBO, underlining the intensification of the AH. Looking at the QBO-E conditions, two maxima appear above the East/North Asia and the West Europe. This correlation with the AH is mainly due to the trapping of the tropical air masses by the anticyclonic circulation which is the mechanism responsible for the formation of low ozone pockets during winter [*Harvey et al.*, 2008]. For a very deep tropical intrusion, the PV value is low and consequently, the tropical air mass maintains its PV signature several days into the AH. The tropical air masses trapped into the AH come from South West Asia where the second maximum appears. However, in this region, tropical air masses can either be quickly advected to high latitudes or, on the contrary, remain confined to low latitudes.

[51] The March/April period, corresponding to the Winter/Summer transition, is shown in Figure 12. The frequency of tropical intrusions globally is lower than for the January/

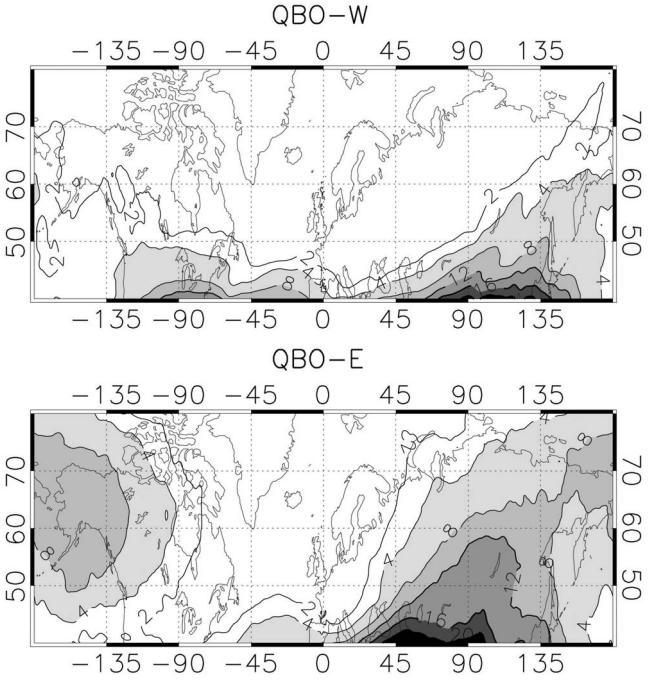

Figure 12. As for Figure 11 but for the March–April period. The shaded contours are higher than 4%.

February period. At the statistical main location of the AH, maximum value is not much higher than 8%. The frequencies are also higher for QBO-E conditions than for QBO-W. Near 40°N, the highest frequencies (greater than 4%) are distributed in the [135°W–180°E] ([45°W–180°E]) longitude range for the QBO-W (QBO-E) cases respectively. The maximum frequency location at 40°N previously identified (Figure 11) appears in the same longitudinal range for both QBO-W and QBO-E. This region which includes frequency values higher than 16% where the dipolar cells have been detected (Figures 8 and 9), is similarly located around 120°E for QBO-W and 80°E for QBO-E conditions. The QBO-E high frequency region shows that the tropical intrusions are more easily advected poleward than under QBO-W conditions.

[52] However, during the last decade, among the 4 major SSWs, 3 of them in 2003–2004, 2005–2006 and 2007–2008 occurred under QBO-W conditions. This fact should be considered when analyzing the diagrams of tropical intrusion frequency (Figures 11 and 12). The difference seen in the frequency values between the QBO-W (lower) and QBO-E (higher) could partly be attributed to the occurrence of SSWs which lead to the inhibition of planetary wave propagation necessary for tropical intrusions and FrIACs occurrences as we have shown in the section 4.1. We discuss now whether the phase of the QBO could be a significant factor in the occurrence of FrIACs events, in particular considering the wave breaking events.

[53] *Peters and Waugh* [1996] classified the poleward Rossby wave breaking in the upper troposphere/lower stratosphere into two types, following the classification of the equatorward Rossby wave breaking first introduced by *Thorncroft et al.* [1993]. Type 1 (P1) in which the intruded ridges tilt upstream into a thin filament before being advected cyclonically in a cyclonic shear zone, and type 2 (P2) in which the intruded air tilts downstream into a broad filament before it wraps up anticyclonically, in an anticyclonic shear zone. This classification has been established in order to explain the exchanges between the upper tropical troposphere and the lower polar stratosphere (around the 330-K surface). As has been suggested by *Knox and Harvey* [2005], breaking events would be modulated by the background zonal-mean zonal shear induced by the QBO.

[54] Following the argument of *Peters and Waugh* [1996] but for the mid stratosphere, the results show that FrIACs events would be favored by the easterly phase of the QBO, increasing the anticyclonic shear within the midlatitudes westerly belt. Figures 8 and 9 show that FrIACs are initially associated with a P2 breaking event characterized by a filament of low PV advected poleward which wraps up anticyclonically. Furthermore, the wave breaking events during FrIAC are located in an anticyclonic shear zone and near a region of weak zonal wind (see Hövmoller diagrams, Figure 4) in good agreement with the above studies [*Peters and Waugh*, 1996; *Knox and Harvey*, 2005].

5. Summary and Conclusions

[55] Using MLS satellite measurements we have highlighted a new case of FrIAC event in 2007 and compared it to the 2005 event [*Manney et al.*, 2006b]. Mixing ratio values of N_2O, H_2O and O_3 for the 2007 FrIAC are quite similar to those of the 2005 event. However, the duration of the 2007 FrIAC, as diagnosed in long-lived species, is much shorter. The 2007 event arises from a tropical intrusion occurring one month later than in the 2005 case and under the summer polar easterlies. Therefore, the 2007 FrIAC is immediately trapped into the summer circulation during the "anticyclonic phase" before tilting in altitude, in a similar fashion to the 2005 case, in late-May. This phase named "shearing phase" is one and a half months shorter than in 2005 [*Allen et al.*, 2011]. Ozone mixing ratios in the core of the FrIACs rapidly decrease due to chemistry, ten days after the tropical intrusion. These results suggest that further modeling investigations and measurements are necessary to improve our understanding of FrIAC events. In particular, i) the specific chemistry associated with ozone inside the core of the FrIACs, ii) the causes for the different persistence of the FrIAC tracer signatures in 2005 and 2007. Improvements on the chemistry could lead to a better understanding of the ozone depletion associated with FrIACs which could influence the ozone budget in the same way that low ozone pockets do [*Harvey et al.*, 2008].

[56] FrIAC dynamical investigations have been performed for the 2003 [*Lahoz et al.*, 2007], 2005 [*Manney et al.*, 2006b] and 2007 (this study) cases. Using MIMOSA PV calculations and ERA-Interim temperature and wind fields over the entire last decade, we described the stages leading to their development. During an early FSW, planetary wave propagation induces the displacement of the polar vortex at midlatitudes. Wave breaking events then occur in the vicinity of a region of weak zonal wind southward of the "westerly belt" allowing the formation of the dipolar PV cell. Finally the tropical intrusion is quickly advected toward the poles along the mean longitude Aleutian High/Polar Vortex boundary. Then tropical air is trapped in the polar summer easterlies polar circulation.

[57] A climatology of meridional heat flux at 30 hPa in the 45°N–55°N latitude range from January to June and zonal mean zonal wind at 30 hPa and 10 hPa at 60°N enables the evolution of the dynamical conditions over the last decade to be followed. Deep SSWs which occurred in 2000–2001, 2003–2004, 2005–2006 and 2008–2009 are associated with zonal wind circulation reversal propagating down to 30 hPa and lead to the inhibition of the planetary wave upward propagation. The FrIAC years are associated with a persistent planetary wave activity until an early/abrupt FSW without a prior major SSW. Regarding SSWs and wave activity, the 1999–2000 springtime conditions appear to favor FrIAC development. However, the heat flux was half that during 2002–2003, 2004–2005 and 2006–2007 conditions so the wave activity was insufficient to allow the advection of the tropical air mass in the polar region.

[58] Finally, we have investigated the possible link between FrIAC events and the phase of the QBO based on a climatology of tropical intrusions based on January/February and March/April periods. We obtained the highest tropical intrusion frequencies under QBO-E. The three FrIACs identified over the last decade and the two cases in northern spring of 1982 and 1994 (not shown) reported by *Manney et al.* [2006b] occurred also during an easterly QBO phase. Using the arguments of *Peters and Waugh* [1996] applied to the lower stratosphere; we surmised that zonal wind anticyclonic shears between the tropical easterly

circulation and midlatitude "westerly belt" could favor "P2" type wave breaking events.

[59] As a conclusion FrIAC events appear to be able to develop in an early and abrupt FSW if no previous major SSW (which inhibits the planetary wave upward propagation) has occurred and if the QBO is in easterly phase which intensifies the anticyclonic zonal wind shear between the tropics and midlatitudes. The impact of the QBO on the polar stratosphere is currently not well understood, particularly with regard to the associated dynamical processes. Additional studies are needed to improve our understanding of the dynamical mechanisms behind the QBO link. Extending the climatology to cover the period from 1960 using ERA-40 reanalysis from ECMWF outputs is planned, and additional chemical measurements and modeling studies are needed to understand the chemistry within the core of the FrIAC and to evaluate the potential impact of such events on stratospheric chemistry.

[60] **Acknowledgments.** This study has been conducted within the framework of the STRAPOLETE project supported by the "Agence Nationale de la Recherche ANR (STRAPOLETE project ANR 08 BLAN 0300), the "Institut Polaire Paul Emile Victor" (IPEV) and the "Centre National d'Etudes Spatiales (CNES)." Y.O.R. was supported by the Norwegian Research Council (Project Arctic Lis). We thank ETHER for access to database (Pôle thématique du CNES). We acknowledge the EOS-MLS instrument science team for the satellite data and the European Centre for Medium-Range Weather Forecasts for providing the ERA-Interim data. We also thank Xavier Vallières for fruitful discussions and the referees for their thorough comments on the manuscript.

References

Allen, D. R., A. R. Douglass, G. L. Manney, S. E. Strahan, J. C. Krosschell, J. V. Trueblood, J. E. Nielsen, S. Pawson, and Z. Zhu (2011), Modeling the frozen-in anticyclone in the 2005 Arctic summer stratosphere, *Atmos. Chem. Phys.*, *11*, 4557–4576, doi:10.5194/acp-11-4557-2011.

Baldwin, M. P., and J. R. Holton (1988), Climatology of the stratospheric polar vortex and planetary wave breaking, *J. Atmos. Sci.*, *45*, 1123–1142, doi:10.1175/1520-0469(1988)045<1123:COTSPV>2.0.CO;2.

Baldwin, M. P., et al. (2001), The quasi-biennial oscillation, *Rev. Geophys.*, *39*, 179–229, doi:10.1029/1999RG000073.

Coy, L., S. Eckermann, and K. Hoppel (2009), Planetary wave breaking and tropospheric forcing as seen in the stratospheric sudden warming of 2006, *J. Atmos. Sci.*, *66*, 495–507, doi:10.1175/2008JAS2784.1.

Dee, D. P., et al. (2011), The ERA-Interim reanalysis: Configuration and performance of the data assimilation system, *Q. J. R. Meteorol. Soc.*, *137*, 553–597, doi:10.1002/qj.828.

Durry, G., and A. Hauchecorne (2005), Evidence for long-lived polar vortex air in the mid-latitude summer stratosphere from in situ laser diode CH_4 and H_2O measurements, *Atmos. Chem. Phys.*, *5*, 1467–1472, doi:10.5194/acp-5-1467-2005.

Froidevaux, L., et al. (2008), Validation of Aura Microwave Limb Sounder stratospheric ozone measurements, *J. Geophys. Res.*, *113*, D15S20, doi:10.1029/2007JD008771.

Gray, L. J., S. Crooks, C. Pascoe, S. Sparrow, and M. Palmer (2004), Solar and QBO influences on the timing of stratospheric sudden warmings, *J. Atmos. Sci.*, *61*, 2777–2796, doi:10.1175/JAS-3297.1.

Harvey, V. L., and M. H. Hitchman (1996), A climatology of the Aleutian High, *J. Atmos. Sci.*, *53*, 2088–2101, doi:10.1175/1520-0469(1996)053<2088:ACOTAH>2.0.CO;2.

Harvey, V. L., R. B. Pierce, T. D. Fairlie, and M. H. Hitchman (2002), A climatology of stratospheric polar vortices and anticyclones, *J. Geophys. Res.*, *107*(D20), 4442, doi:10.1029/2001JD001471.

Harvey, V. L., C. E. Randall, G. L. Manney, and C. S. Singleton (2008), Low-ozone pockets observed by EOS-MLS, *J. Geophys. Res.*, *113*, D17112, doi:10.1029/2007JD009181.

Hauchecorne, A., S. Godin, M. Marchand, B. Heese, and C. Souprayen (2002), Quantification of the transport of chemical constituents from the polar vortex to midlatitudes in the lower stratosphere using the high-resolution advection model MIMOSA and effective diffusivity, *J. Geophys. Res.*, *107*(D20), 8289, doi:10.1029/2001JD000491.

Hitchman, M. H., and A. S. Huesmann (2007), A seasonal climatology of Rossby wave breaking in the 320–2000 K layer, *J. Atmos. Sci.*, *64*, 1922–1940, doi:10.1175/JAS3927.1.

Holton, J. R., and H.-C. Tan (1980), The influence of the equatorial quasi-biennial oscillation on the global circulation at 50 mb, *J. Atmos. Sci.*, *37*, 2200–2208, doi:10.1175/1520-0469(1980)037<2200:TIOTEQ>2.0.CO;2.

Holton, J. R., and H.-C. Tan (1982), The quasi-biennial oscillation in the Northern Hemisphere lower stratosphere, *J. Meteorol. Soc. Jpn.*, *60*, 140–148.

Hoor, P., H. Fischer, L. Lange, J. Lelieveld, and D. Brunner (2002), Seasonal variations of a mixing layer in the lowermost stratosphere as identified by the CO-O3 correlation from in situ measurements, *J. Geophys. Res.*, *107*(D5), 4044, doi:10.1029/2000JD000289.

Huret, N., M. Pirre, A. Hauchecorne, C. Robert, and V. Catoire (2006), On the vertical structure of the stratosphere at midlatitudes during the first stage of the polar vortex formation and in the polar region in the presence of a large mesospheric descent, *J. Geophys. Res.*, *111*, D06111, doi:10.1029/2005JD006102.

Jacobi, C., D. Kürschner, H. G. Muller, D. Pancheva, N. J. Mitchell, and B. Naujokat (2003), Response of the mesopause region dynamics to the February 2001 stratospheric warming, *J. Atmos. Sol. Terr. Phys.*, *65*, 843–855, doi:10.1016/S1364-6826(03)00086-5.

Knox, J. A., and V. L. Harvey (2005), Global climatology of inertial instability and Rossby wave breaking in the stratosphere, *J. Geophys. Res.*, *110*, D06108, doi:10.1029/2004JD005068.

Lahoz, W. A., A. J. Geer, and Y. J. Orsolini (2007), Northern Hemisphere stratospheric summer from MIPAS observations, *Q. J. R. Meteorol. Soc.*, *133*, 197–211, doi:10.1002/qj.24.

Lambert, A., et al. (2007), Validation of the Aura Microwave Limb Sounder middle atmosphere water vapour and nitrous oxide measurements, *J. Geophys. Res.*, *112*, D24S36, doi:10.1029/2007JD008724.

Liu, Y., C. X. Liu, H. P. Wang, X. X. Tie, S. T. Gao, D. Kinnison, and G. Brasseur (2009), Atmospheric tracers during the 2003–2004 stratospheric warming event and impact of ozone intrusions in the troposphere, *Atmos. Chem. Phys.*, *9*, 2157–2170, doi:10.5194/acp-9-2157-2009.

Livesey, N. J., et al. (2007), Version 2.2 level 2 data quality and description document, *Tech. Rep. JPL D-33509*, Jet Propul. Lab., Pasadena, Calif.

Lu, H., M. P. Baldwin, L. J. Gray, and M. J. Jarvis (2008), Decadal-scale changes in the effect of the QBO on the northern stratospheric polar vortex, *J. Geophys. Res.*, *113*, D10114, doi:10.1029/2007JD009647.

Manney, G., L. Froidevaux, J. Waters, R. Zurek, J. Gille, J. Kumer, J. Mergenthaler, A. Roche, A. O'Neill, and R. Swinbank (1995), Formation of low-ozone pockets in the middle stratospheric anticyclone during winter, *J. Geophys. Res.*, *100*(D7), 13,939–13,950, doi:10.1029/95JD00372.

Manney, G. L., K. Krüger, J. L. Sabutis, S. A. Sena, and S. Pawson (2005), The remarkable 2003–2004 winter and other recent warm winters in the Arctic stratosphere since the late 1990s, *J. Geophys. Res.*, *110*, D04107, doi:10.1029/2004JD005367.

Manney, G. L., M. L. Santee, L. Froidevaux, K. Hoppel, N. J. Livesey, and J. W. Waters (2006a), EOS MLS observations of ozone loss in the 2004–2005 Arctic winter, *Geophys. Res. Lett.*, *33*, L04802, doi:10.1029/2005GL024494.

Manney, G. L., N. J. Livesey, C. J. Jimenez, H. C. Pumphrey, M. L. Santee, I. A. MacKenzie, and J. W. Waters (2006b), EOS Microwave Limb Sounder observations of "frozen-in" anticyclonic air in Arctic summer, *Geophys. Res. Lett.*, *33*, L06810, doi:10.1029/2005GL025418.

Manney, G. L., et al. (2009), Satellite observations and modeling of transport in the upper troposphere through the lower mesosphere during the 2006 major stratospheric sudden warming, *Atmos. Chem. Phys.*, *9*, 4775–4795, doi:10.5194/acp-9-4775-2009.

Marchand, M., S. Godin, A. Hauchecorne, F. Lefèvre, S. Bekki, and M. Chipperfield (2003), Influence of polar ozone loss on northern midlatitude regions estimated by a high-resolution chemistry transport model during winter 1999/2000, *J. Geophys. Res.*, *108*(D5), 8326, doi:10.1029/2001JD000906.

McIntyre, M. E., and T. N. Palmer (1983), Breaking planetary-waves in the stratosphere, *Nature*, *305*, 593–600, doi:10.1038/305593a0.

McIntyre, M. E., and T. N. Palmer (1984), The surf zone in the stratosphere, *J. Atmos. Terr. Phys.*, *46*, 825–849, doi:10.1016/0021-9169(84)90063-1.

Naito, Y., and I. Hirota (1997), Interannual variability of the northern winter stratospheric circulation related to the QBO and the solar cycle, *J. Meteorol. Soc. Jpn.*, *75*, 925–937.

Naoe, H., and K. Shibata (2010), Equatorial quasi-biennial oscillation influence on northern winter extratropical circulation, *J. Geophys. Res.*, *115*, D19102, doi:10.1029/2009JD012952.

Orsolini, Y. J. (2001), Long-lived tracer patterns in the summer polar stratosphere, *Geophys. Res. Lett.*, *28*(20), 3855–3858, doi:10.1029/2001GL013103.

Orsolini, Y. J., J. Urban, D. P. Murtagh, S. Lossow, and V. Limpasuvan (2010), Descent from the polar mesosphere and anomalously high stratopause observed in 8 years of water vapor and temperature satellite observations by the Odin Sub-Millimeter Radiometer, *J. Geophys. Res.*, *115*, D12305, doi:10.1029/2009JD013501.

Peters, D., and D. W. Waugh (1996), Influence of barotropic shear on the poleward advection of upper tropospheric air, *J. Atmos. Sci.*, *53*, 3013–3031, doi:10.1175/1520-0469(1996)053<3013:IOBSOT>2.0.CO;2.

Ray, E., F. Moore, J. Elkins, G. Dutton, D. Fahey, H. Vömel, S. Oltmans, and K. Rosenlof (1999), Transport into the Northern Hemisphere lowermost stratosphere revealed by in situ tracer measurements, *J. Geophys. Res.*, *104*(D21), 26,565–26,580, doi:10.1029/1999JD900323.

Schwartz, M. J., et al. (2008), Validation of the Aura Microwave Limb Sounder temperature and geopotential height measurements, *J. Geophys. Res.*, *113*, D15S11, doi:10.1029/2007JD008783.

Thorncroft, C. D., B. J. Hoskins, and M. E. McIntyre (1993), Two paradigms of baroclinic-wave life-cycle behaviour, *Q. J. R. Meteorol. Soc.*, *109*, 737–761.

Tomikawa, Y. (2010), Persistence of easterly wind during major stratospheric sudden warmings, *J. Clim.*, *23*, 5258–5267, doi:10.1175/2010JCLI3507.1.

Waters, J. W., et al. (2006), The Earth Observing System Microwave Limb Sounder (EOS MLS) on the Aura satellite, *IEEE Trans. Geosci. Remote Sens.*, *44*, 1075–1092, doi:10.1109/TGRS.2006.873771.

Waugh, D. W. (1996), Seasonal variation of isentropic transport out of the tropical stratosphere, *J. Geophys. Res.*, *101*(D2), 4007–4023, doi:10.1029/95JD03160.

M.-A. Drouin, N. Huret, and R. Thiéblemont, Laboratoire de Physique et Chimie de l'Environnement et de l'Espace/CNRS, Université d'Orléans, 3A Ave. de la Recherche scientifique, Orléans F-45071, France. (marc-antoine.drouin@cnrs-orleans.fr; nathalie.huret@cnrs-orleans.fr; remi.thieblemont@cnrs-orleans.fr)

A. Hauchecorne, LATMOS, Quartier des Garennes, 11 Blvd. d'Alembert, Guyancourt F-78280, France. (alain.hauchecorne@latmos.ipsl.fr)

Y. J. Orsolini, NILU, PO Box 100, N-2027 Kjeller, Norway. (yvan.orsolini@nilu.no)